

Effect of Step Depth and Angle in Kline-Fogleman (Kfm-2) Airfoil

Fadi Mishriky¹ and Paul Walsh²

¹ Ryerson University, Toronto, Canada

Received: 10 December 2015 Accepted: 31 December 2015 Published: 15 January 2016

Abstract

Recent years have witnessed extensive research efforts that aim at improving the aerodynamic performance of aircraft. While most of the efforts are drawn towards high-lift systems, simple and innovative designs like Gurney flaps, trapped vortex cavities and backward-facing steps can have a significant effect on enhancing the aerodynamic properties of airfoils. One of those simple ideas is the Kline-Fogleman modified airfoil (KFm-2), which is basically an airfoil with a backward-facing step on the upper surface located at midway the chord length. It is claimed that the step creates a low pressure recirculation region on the suction side of the airfoil that may enhance the lifting force. This study will numerically examine the ability of the KFm-2 design to enhance the lift and drag properties of a NACA 2412 at a high Reynolds number of 5.9×10^6 . The effect of the step depth and the step angle will be thoroughly examined.

Index terms— aerodynamics, stepped airfoil, backward-facing step, KFm-2 airfoil, CFD.

1 I. Introduction

The majority of aircraft today use high-lift systems to augment the wing's lifting capabilities at different flight regimes. The importance of these systems is emphasized during take-off and landing, when the wings are required to generate high lifting forces at minimal speeds. These hinged surfaces are employed in most commercial subsonic aircraft and controlled using heavy mechanical devices as pistons, screws, racks and pinions, etc. All these components add to the cost, mass and complexity of the aircraft. Wlezien et al. [1] stated that half the cost and complexity of an aircraft wing are due to the complexity of the high-lift system. In addition, the gaps between the surface and the wing significantly increase the drag forces and the noise. For these reasons, any less complex and innovative design should be examined.

One of the simplest potential solutions is a series of stepped airfoils designed by Kline and Fogleman (KFm-series). In the early 1960s, Richard Kline, who had the hobby of making paper airplanes, created a paper airplane design that could fly for long distances despite wind or turbulences.

He presented the paper airplane to his colleague Floyd Fogleman who saw that this model can fly and resist stalling. The two men then filed a U.S. patent for a wedged-like airfoil that is hollow from below [2], and with further developments, they filed another patent in 1977 [3] for an airfoil with a backward-facing step on the pressure side, with one or more membranes pivotally hinged near the step. A new family of airfoils (KFm1 -KFm8) diverged from their patented designs, where backward-facing steps were installed on either side of the airfoil. The KFm airfoils gained popularity among the radio controlled airplane community from that time to date, with most users claiming better stability and enhanced aerodynamic performance. The step is supposed to intentionally separate the flow from the airfoil, and trap a recirculating vortex over its vicinity. This recirculating zone creates low pressure regimes on specific locations of the airfoil, and this may enhance the aircraft performance.

Inspired by the Kline-Fogleman airfoil designs, Fertis et al. [4] designed an airfoil with a backward-facing step on the upper surface of the airfoil, and they filed a U.S. patent for their design titled "Airfoil". Six years later, Fertis [5] published the experimental results of the design shown in his patent. The experimental tests

were performed on NACA 23012 airfoil at a range of Reynolds numbers from $1e+5$ to $5.5e+5$, and a wide range of angle of attacks; from 2° to 38° . The results showed improved stall characteristics at all tested airspeeds, increased lift coefficients and increased functional lift-to-drag ratios over a range of angle of attacks. Fathi et al. [6] performed a number of experimental and numerical experiments at a Reynolds Number of $5e+5$ on 15 different configurations of a symmetric NACA 0012 airfoil with a backward-facing step on either sides. The results showed that a step on the lower side of the airfoil whose depth is half the thickness of the airfoil and extends to the trailing edge will increase the lift and the lift to drag ratio. For all other cases, especially when the step is on the upper surface, the drag coefficient significantly increases and leads to a drop in the lift to drag ratio. Cox et al. [7] compared the Rolf Girsberger (RG) -15 airfoil section with a KFM-2 step with the clean RG-15 airfoil at four low Reynolds Numbers between $2.8e+3$ and $1e+5$. Results revealed that at these Reynolds number, the addition of the KFM-2 step was found to have no useful aerodynamic benefits.

With most of the studies were performed at low Reynolds numbers, this paper will investigate the capabilities of the KFM-2 approach to enhance the aerodynamic performance of a NACA 2412 airfoil at a high Reynolds number of $5.9e+6$. The KFM-2 airfoil employs a backward-facing step at the mid-chord location on the suction side of the airfoil as shown Figure 1. This design is commonly encountered in cases of sliding morphing skins. In such designs, two rigid surfaces remain in contact and slide against each other during morphing. This interface introduces backwardfacing steps on the wings' surface. The study will offer an in-depth numerical investigation on the effect of the step depth and the step angle on the aerodynamic properties of the airfoil. First, the numerical methodology and amesh independence study will be presented. The numerical testing will focus on variation of the lift coefficient C_L and the drag coefficient C_D with different step configurations. Finally, conclusion about the aerodynamics of the KFM-2 airfoil will be presented with general recommendations about the step depth and angle.

II. Numerical Modeling and Boundary conditions

The commercial CFD code FLUENT is used in this study to simulate the flow using the finite volume method. An implicit density-based solver is used to solve the Navier-Stokes and the turbulence transport equations, where the convective and diffusive fluxes were calculated using a second-order Upwind scheme, and the gradients of scalar quantities were reconstructed using the Least-Squares cell-based method. The turbulence of the flow is modeled using the four equations Langtry-Menter transitional SST turbulence model [8,9]. This model has been shown to accurately model the transition of the viscous boundary layer from laminar to turbulent which was observed to have an effect on the value of the lift and drag coefficients.

The airfoil used in the study is a standard NACA 2412 airfoil with a sharp trailing edge, a unity chord length and a computational domain that extends 32 chords in a C-grid topology. The air is treated as an ideal gas whose viscosity is calculated using the three equations Sutherland's formula.

The baseline parameters of the airfoil are from the NACA 2412 with a vertical step at the mid-chord with depth of 0.015 chord lengths. The NACA profile continues after the step, but scaled along the Y direction to intersect the step at its lower edge.

The mesh that discretizes the computational domain must compromise between computational accuracy and run time. To fulfill this challenging demand, a mesh independent study is performed using a family of three consecutively refined meshes with a constant refinement factor of $r = 2$. This means that for 2D meshes, the number of cells is quadrupled from each mesh to next refined one. The coarse, medium and fine meshes consist of 12,000, 48,000 and 192,000 cells, respectively. The Richardson's extrapolation method [10] is used to calculate the continuum value C_{cont} , where r is an aerodynamic property that is evaluated on the coarse, medium and fine meshes to obtain C_{coarse} , C_{medium} and C_{fine} respectively. In our case the lift coefficient C_L was used for this analysis. The continuum value C_{cont} is calculated as follows:

3 Global

$$C_{cont} = \frac{C_{fine} - r^2 C_{medium}}{1 - r^2} + \frac{C_{medium} - r C_{coarse}}{1 - r} \quad (1)$$

where r is the refinement ratio, and in our case it is constant at 2. While p is the observed order of accuracy of the solution and is calculated as:

$$p = \frac{\log(C_{medium} - C_{coarse})}{\log(r)} \quad (2)$$

Equations (1-3) were used to calculate the continuum value C_{cont} of the lift coefficient. Figure 2 shows the values obtained from three meshes as well as the extrapolated continuum value. The value obtained from the fine mesh was 0.244% away from the asymptotic value C_{cont} . This shows the adequacy of the fine mesh to capture the important physical features of the flow, and further refinements will only increase the computational time without notable improvement in the numerical accuracy. Thus, the fine mesh will be used in the next section to examine the effect of the step depth and angle on the aerodynamic performance of KFM-2 airfoil with a NACA 2412 profile. In this subsection, the effect of the step depth on the lift and drag coefficients of the airfoil will be tested. The flow is directed with an angle of attack of 2.5° over the NACA 2412 airfoil that has a vertical step. The location of the step is fixed at the mid chord length ($x/c = 0.5$), and the only variable will be the step

104 depth. The testing starts with a step of depth $h/c = 0.0075$ and increase to $h/c = 0.025$ with an
 105 increment of 0.0025 from one configuration to the other. Figure 3 shows the two extreme positions of the step
 106 depths representing $h/c = 0.0075$ and $h/c = 0.025$, where h is the step depth and c is the
 107 chord length. Eight configurations of different step depths were numerically simulated until convergence. The
 108 convergence criterion was judged by the complete stability of the lift, drag and moment coefficients.

109 4 III. Results and Discussion

110 $C_L = C_{L,c} + C_{L,p} + C_{L,v}$ (2)

111 As the depth gradually increased from $h/c = 0.0075$ to $h/c = 0.025$, the lift coefficient decreased
 112 by about 20%, and the highest value of lift coefficient obtained (0.4812), is lower than the value obtained by the
 113 unchanged (clean) NACA 2412 which is equal to 0.5172. Figure 4 shows the inverse relation between the lift
 114 coefficient C_L and the step depth h/c . The steep slope of the curve in Figure 4 reflects the strong correlation
 115 between the step depth and lifting forces on the airfoil. To study the relation between the lifting forces and the
 116 step depth, the pressure distribution over the eight configurations of step depths is shown in Figure 5. The step
 117 caused the airfoil thickness to locally decrease, which resulted in a deceleration of the flow as it traveled past the
 118 step, consequently increasing the value of the pressure after the step. As the step depth increased, the pressure
 119 increased on the suction side leading to an overall drop in the lift coefficient values.

120 It was also observed that the step depth affected the pressure distribution upstream the step. Thus, from this
 121 analysis, it could be concluded that an increase in the step depth will cause the lifting forces to decrease.

122 Next, a similar analysis was performed to establish the relation between the drag coefficient and depth of the
 123 installed step. Results of this analysis are shown in Figure 6. A linear-like relation is observed between the step
 124 depth h/c and the value of the drag coefficient of the airfoil. The lowest value of drag coefficient is still higher
 125 than the value obtained from the clean NACA 2412 at the same conditions. The drag coefficient value of a clean
 126 NACA 2412 is 0.00515, while the lowest drag coefficient in Figure 6 is observed at a step depth of 0.0075 , and
 127 is equal to 0.00668.

128 A nearly constant increment of 0.0015 in the drag coefficient value is observed with each 0.0025 increment
 129 in the step depth. This relation holds over the full testing range. To study this direct relation, the drag coefficient
 130 is decomposed to its two main components; the pressure drag coefficient and the viscous drag coefficient. Equation
 131 4 provides the expression used to calculate each component. $C_D = C_{D,p} + C_{D,v}$ (4)

132 airfoil surface. The results of this decomposition is shown in Figure 7.

133 Where $C_{D,p}$ is the pressure drag coefficient, $C_{D,v}$ is the friction drag coefficient or viscous drag coefficient, ρ is
 134 the fluid density, v is the reference velocity, A is the reference area, p is the pressure at the surface dA , p_0 is
 135 the reference pressure, n is a unit vector normal to the surface dA , τ_w is the wall shear stresses at the surface
 136 dA and t is a unit vector tangent to the surface dA . The pressure drag coefficient is calculated as the surface
 137 integration of the pressure coefficient value acting normal to the airfoil surface, while the viscous drag component
 138 is the surface integration of the skin friction coefficient along the tangential direction of the The viscous drag
 139 coefficient experienced a small increase from one step depth to the other. On the other hand, the pressure drag
 140 coefficient is the dominant factor, and its contribution increased with the increase of the step depth. This is
 141 mainly due to the nature of the drag coefficient of stepped airfoils which is driven by the interaction of the low
 142 pressure region at the recirculation zone with the vertical wall of the step. With the increase of the step depth,
 143 the pressure experiences a slight increase, but the exposed area of the airfoil noticeably increases. This results in
 144 a constant increase in the pressure drag force acting on the step from one depth to the other. For that reason,
 145 the drag coefficient continuously increased as the step depth increased. The previous subsection showed a strong
 146 correlation between the step depth and the values of the lift and drag coefficients. This subsection focuses on the
 147 effect of the KFM-2 step angle on the aerodynamic properties studied in the previous section.

148 Figure 8 shows five different configurations of the airfoil with the step angle rotated at different angles.

149 In all cases the step is fixed at $X=0.5 C$, with a step depth of $D U = 0.015 C$, while the step angle θ changes
 150 from 45° to -45° , with the zero at the vertical position and positive angles are in the counter-wise direction.
 151 The flow was set to an angle of attack of 2.5° in the simulations and the complete stability of the lift and drag
 152 coefficients marked the convergence of the solution. Table 1 shows the lift and drag coefficients calculated at
 153 different step configurations. (a)

154 The five cases obtained nearly the same values for the lift and drag coefficients. This is confirmed by the
 155 identical values of the pressure distribution and the shear wall stresses shown in Figure 9a and 9b respectively.
 156 The identical curves justifies the equal results of the five configurations. A small difference is observed in the lift
 157 to drag ratio C_L/C_D in case of the angle $\theta=45^\circ$. This is due to the small displacement of the recirculation
 158 zone to the lower corner of the inclined step. In cases of step angles from $\theta=-45^\circ$ to 22.5° the recirculation zone
 159 started at $X/C = 0.513$, while in case of $\theta=45^\circ$, the bottom corner of the step started at $X/C = 0.517$, which is the
 160 location that marks the beginning of the recirculation zone. For that reason, the case with a step angle of $\theta=45^\circ$
 161 obtained a slightly higher drag coefficient and lower lift coefficient when compared to the other cases. For cases
 162 with negative step angles, the additional space located at the cavity of the inclined step is filled with a cascade
 163 of minute low energy vortices that have negligible effect on the aerodynamics of the flow. Therefore, the effect
 164

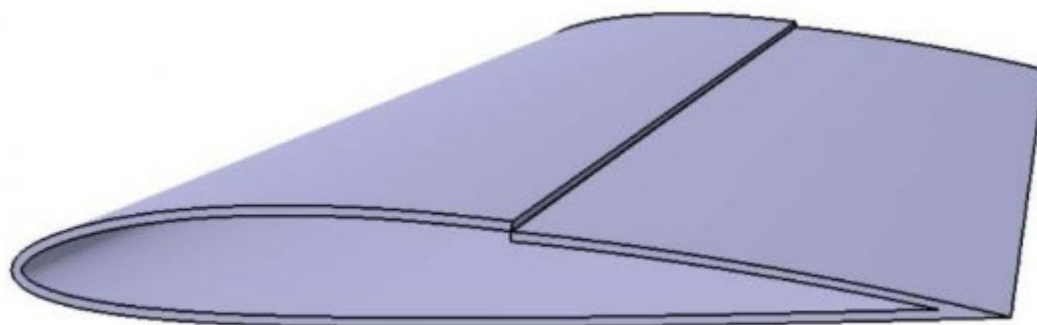
165 of the step angle ? ranging between 45 to-45° could be neglected in the aerodynamic analysis of backward-facing
166 steps installed on the upper surfaces of airfoils.

167 5 IV. Conclusion

168 This study examined the aerodynamic performance of the Kfm-2 airfoil with a NACA 2412 profile. Different
169 variations of this design were achieved by changing the step depth and the step angle employed at the upper
170 surface of the airfoil. The flow was simulated numerically at a Reynolds number of 5.9e+6, a Mach number of
171 0.16 and angle of attack of 2.5°. The study showed that employing a step on the upper surface of a NACA 2412
172 airfoil has degraded the aerodynamic performance in terms of the values of the lift and drag coefficients. The
173 lift coefficient decreased as the step depth increased, while the drag coefficient followed a linear-like behavior
174 that increased constantly as the step depth increased. Decomposition of the drag coefficient to its two main
175 components revealed that for stepped airfoils, the pressure drag coefficient dominates the calculation of the drag
176 forces due to the interaction of the low pressure recirculation zone with the 'vertical' wall of the step. Changing
177 the angle of the step from 45° to -45° did not have any effect on the drag and lift coefficients. Thus, employing
178 a backward-facing step on the upper surface of a NACA 2412 at a high Reynolds number of 5.9e6 has degraded
179 the aerodynamic performance when compared to the unchanged airfoil. However, decreasing the step depth
180 diminishes these adverse effects.

181 6 Global Journal of Researches in Engineering

() Volume XVI Iss J ^{1 2}



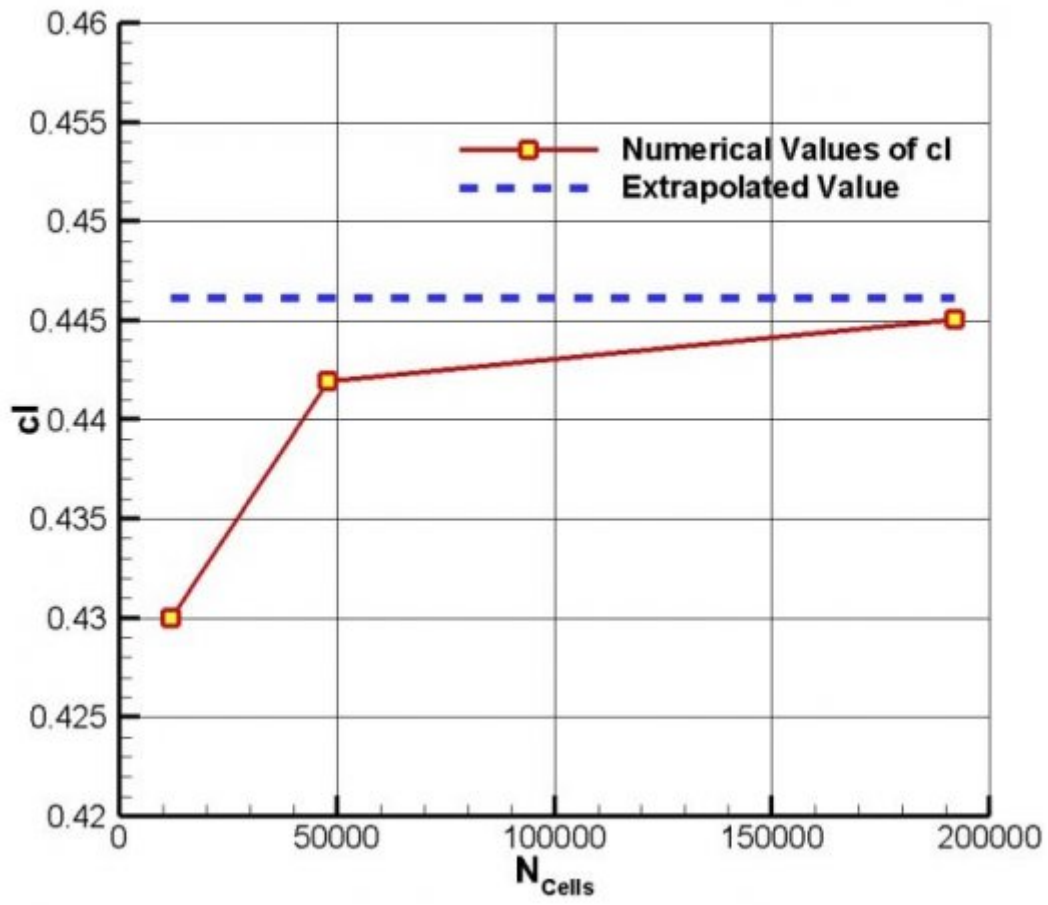
1

Figure 1: Figure 1 :

182

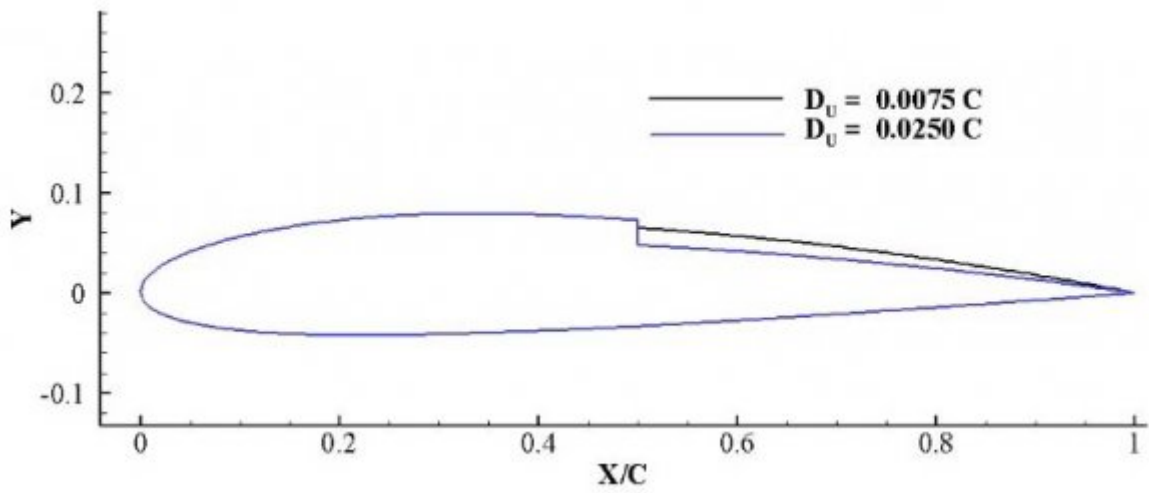
¹© 2016 Global Journals Inc. (US)

²Effect of Step Depth and Angle in Kline-Fogleman (Kfm-2) Airfoil © 2016 Global Journals Inc. (US)



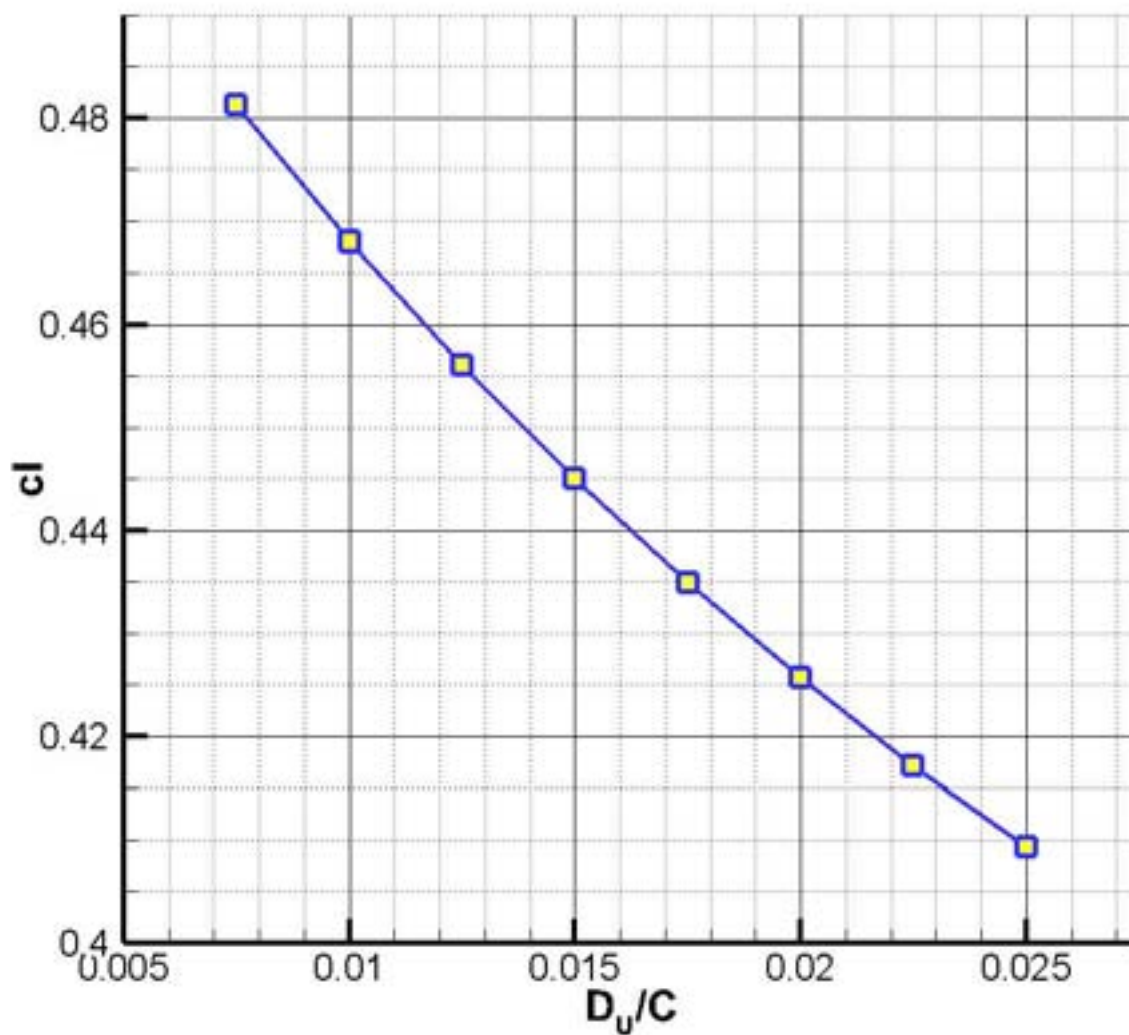
2

Figure 2: Figure 2 :



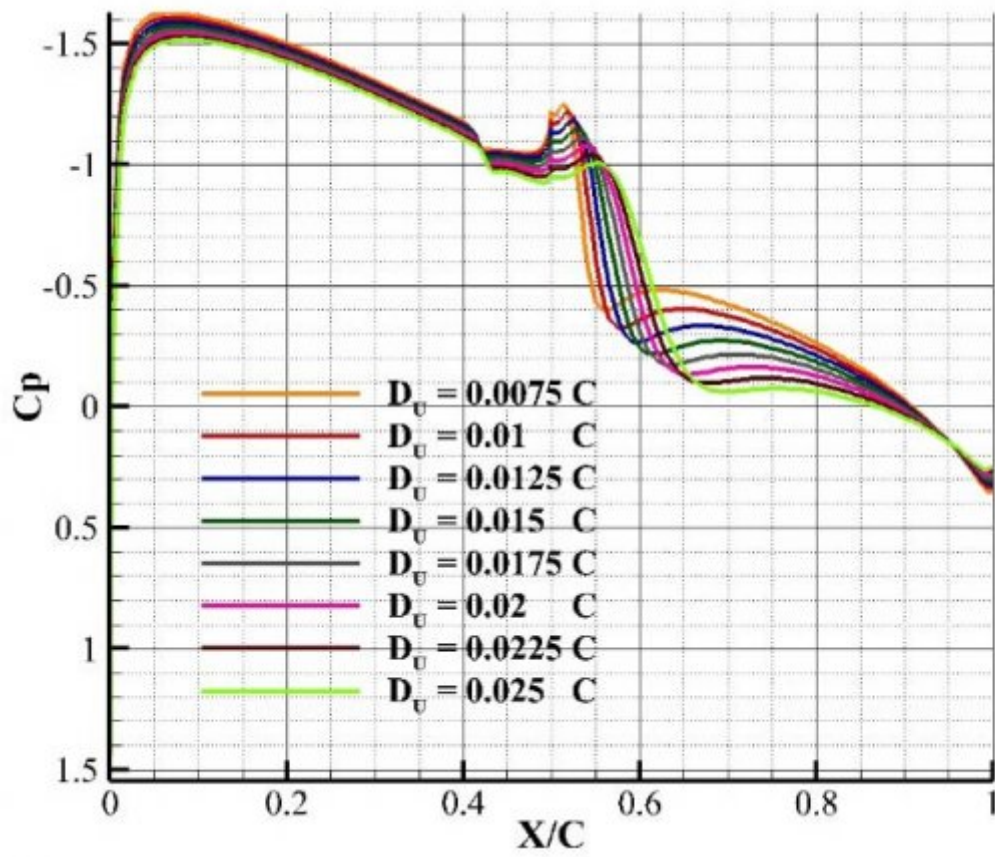
3

Figure 3: Figure 3 :



4

Figure 4: Figure 4 :



5

Figure 5: Figure 5 :

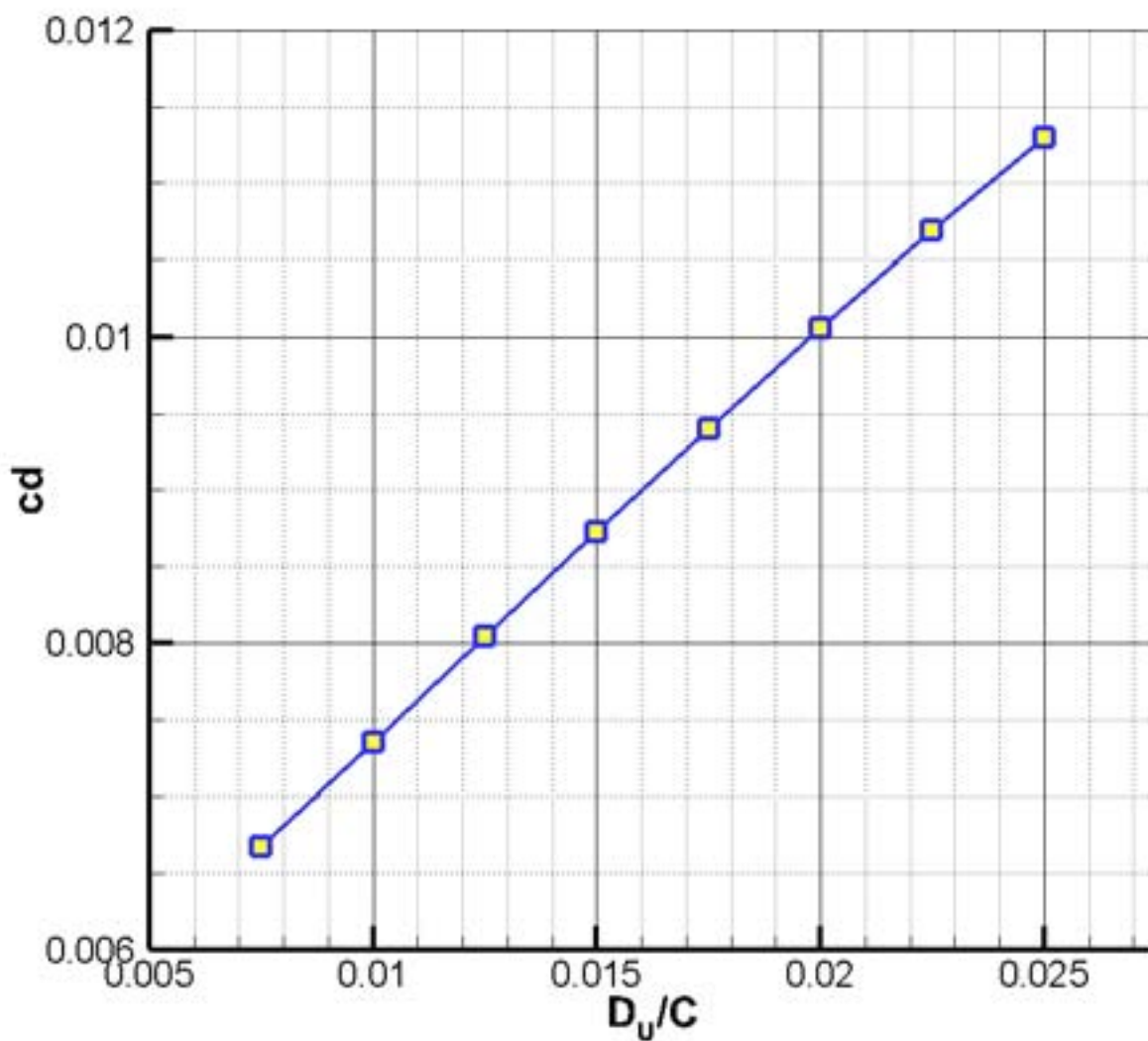
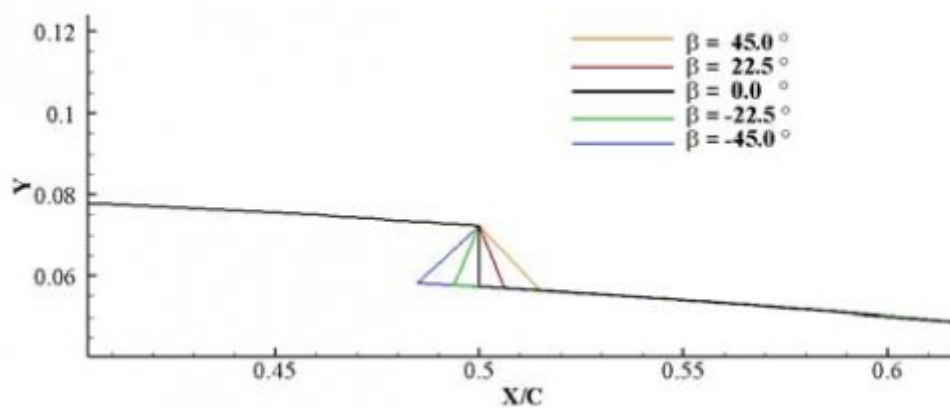


Figure 6:



6

Figure 7: Figure 6 :

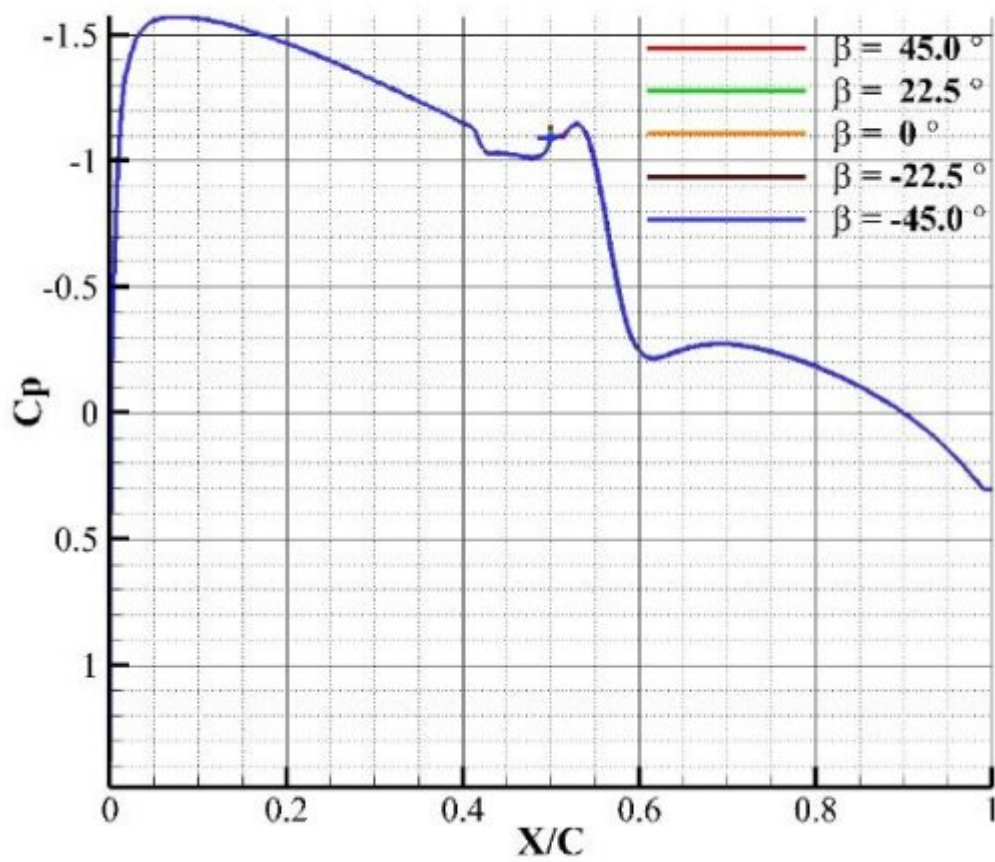
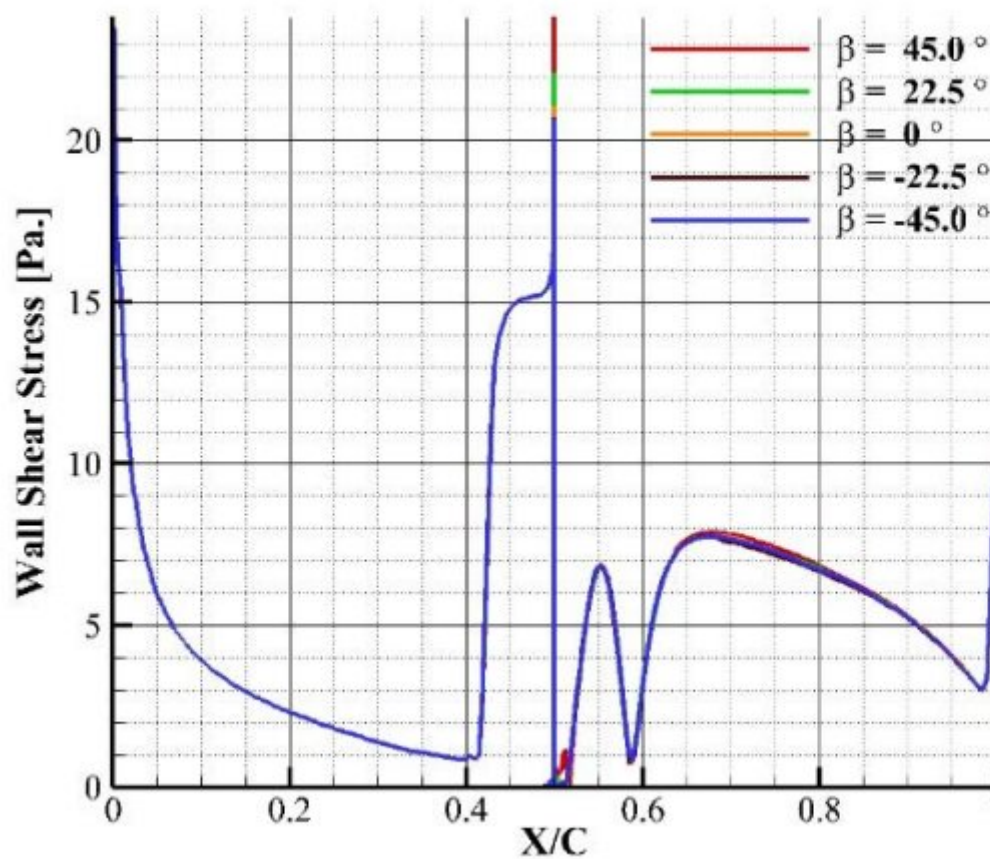


Figure 8:



7

Figure 9: Figure 7 :

1

Effect

Figure 10: Table 1 :

-
- 183 [Kline and fogleman (ed.) ()] , R L Kline , F F & fogleman . No. 3706430. U.S. Patent and Trademark Office
184 (ed.) 1972. Washington, DC. (U.S. Patent)
- 185 [Kline and Fogleman (ed.) ()] , R L Kline , F F Fogleman . U.S. Patent and Trademark Office (ed.) 1977.
186 Washington, DC. 046.
- 187 [Fertis and Smith (ed.) ()] , D G Fertis , L L Smith . U.S. Patent and Trademark Office (ed.) 1986. Washington,
188 DC. 606.
- 189 [Finaish and Witherspoon ()] ‘Aerodynamic performance of an airfoil with step-induced vortex for lift augmen-
190 tation’. F Finaish , S Witherspoon . *Journal of Aerospace Engineering* 1998. 11 (1) p. .
- 191 [Australasian Fluid Mechanics Conference] *Australasian Fluid Mechanics Conference*, (Melbourne, Australia)
192 RMIT University
- 193 [Langtry and Menter ()] ‘Correlationbased transition modeling for unstructured parallelized computational fluid
194 dynamics codes’. R B Langtry , F R Menter . *AIAA journal* 2009. 47 (12) p. .
- 195 [Shyy et al. ()] ‘Evaluation of Richardson extrapolation in computational fluid dynamics’. W Shyy , M Garbey
196 , A Appukuttan , J Wu . *Numerical Heat Transfer: Part B: Fundamentals* 2002. 41 (2) p. .
- 197 [Fertis ()] ‘New airfoil-design concept with improved aerodynamic characteristics’. D G Fertis . *Journal of*
198 *Aerospace Engineering* 1994. 7 (3) p. .
- 199 [Cox et al. (2014)] ‘Performance of a Stepped Airfoil at Low Reynolds Numbers’. M J Cox , V Avakian , B P
200 Huynh . *Proceedings of the 19th*, (the 19th) 2014. December.
- 201 [Menter et al. ()] *Transition modelling for general purpose CFD codes. Flow, Turbulence and Combustion*, F R
202 Menter , R Langtry , S Völker . 2006. 77 p. .
- 203 [Wlezien et al. ()] R W Wlezien , G C Homer , A R Mcgowan , S L Padula , M A Scott , R J Silcox , J O
204 Simpson . *The Aircraft Morphing Program. AIAA Paper*, 1998. p. .